Available online at www.sciencedirect.com
ScienceDirect
Applied Soft Computing 8 (2008) 937–948
Applied Soft Computing
www.elsevier.com/locate/asoc

Direct adaptive neural flight control system for an unstable unmanned aircraft

S. Suresh [a,*], N. Kannan [b]

[a] School of Electrical and Electronics Engineering, Nanyang Technological University, Singapore
[b] Department of Engineering, University of Leicester, UK

Received 22 December 2006; received in revised form 29 May 2007; accepted 28 July 2007
Available online 3 August 2007

Abstract

A direct adaptive controller design using neural network is proposed for an unstable unmanned research aircraft similar in configuration to combat aircraft. The control law to track the pitch rate command is developed based on system theory. Neural network with linear filters and back propagation through time learning algorithm is used to approximate the control law. The bounded signal requirement to develop the neural controller is circumvented using an off-line finite time training scheme, which provides the necessary stability and tracking performances. On-line learning scheme is implemented to compensate for uncertainties due to variation in aerodynamic coefficients, control surface failures and also variations in center of gravity position. The performance of the proposed control scheme is validated at different flight conditions. The disturbance rejection capability of the neural controller is analyzed in the presence of the realistic gust and sensor noises. Hardware-in-loop simulation is also carried out to study the behavior of control surface deflections in real-time.

Keywords: Neural network; Direct adaptive control scheme; Unmanned aircraft; Flight control system; Hardware-in-loop simulation and disturbance rejection

1. Introduction

Conventional flight control systems are designed using the linearized aircraft models at different equilibrium or trim conditions and the controller gains are scheduled to provide good performance in the complete operating flight envelope [1,2]. However, it is difficult for the gain scheduling technique to provide the necessary tracking performance under severe uncertainty and fault conditions. Adaptive nonlinear flight control schemes offer effective alternatives to overcome this difficulty. Adaptive control research is directed towards nonlinear systems with a special class of parametric uncertainty, which appear linearly with respect to known nonlinearities. Recently, neural networks have been explored for modeling and control of nonlinear systems due to their approximating capabilities and inherent adaptive features. Also, from a practical perspective, massive parallelism and fast adaptability of neural network implementations provide more incentives for further investigation in problems involving systems with unknown uncertainties. The feasibility of applying neural network architectures for nonlinear system identification and control is first demonstrated through numerical simulation studies in [3], where the role of the neural networks is to learn some underlying relationship between the input–output data and also approximate the corresponding control law. Since then, a great deal of progress has been made both in theory and practice of neural network based nonlinear adaptive control system designs [4–10].

One of the areas to receive wide attention with respect to adaptive controller based neural network architectures is flight control system design. Modern day aircraft flight control systems are designed such that they can accommodate stringent flying quality requirements, parameter uncertainties, and component failures. In this context, an adaptive control scheme based on inversion of a linearized plant model is developed in [11], where the inversion errors are compensated through multi-layer perceptron neural networks. The above method is proven to be effective in many applications including systems operating in highly nonlinear aerodynamic regime [11], systems with rapidly varying nonlinear dynamics [12,13] and systems with high levels of uncertainties [14]. Alternatively, direct adaptive control

* Corresponding author.
E-mail addresses: ssundaram@ntu.edu.sg (S. Suresh), kn38@leicester.ac.uk (N. Kannan).

1568-4946/$ – see front matter © 2007 Elsevier B.V. All rights reserved.
doi:10.1016/j.asoc.2007.07.009

system using model inversion technique based on two neural networks is presented for control augmentation system of F-18 aircraft in [15]. In this scheme, the first neural network represents the nominal inverse transformation for feedback linearization, and the second neural network is used to compensate the inversion error. This method has been applied to design a control system in tilt-rotor aircraft [16], and helicopter [17]. In [18,19], it is shown that neural networks with on-line capabilities can adapt to changes in aircraft dynamics undergoing highly nonlinear maneuvers. Use of neural network controller for nonlinear flight control system is summarized in [20]. Apart from nonlinearities and uncertainties, restructurable flight control systems for sensor and actuator failures have also gained attention [21]. Reconfigurable flight control law for tailless aircraft has also been investigated with offline–online learning strategy [21–24] (the reader is referred to [6] for a complete survey of adaptive neural control systems for various applications). The most widely used flight control scheme based on neural networks is the feedback error-learning scheme [9–11,18,19]. In this scheme, the control architecture uses a conventional controller in the inner loop to stabilize the system dynamics, and the neural controller acts as an aid to the conventional controller for compensating any nonlinearities. Under severe modeling uncertainties, fault conditions and time varying nonlinear dynamics of the plant, the neural network is adapted on-line to ensure better tracking ability, provided the conventional controller in the inner loop satisfies the bounded signal requirements. Since the conventional controller is not designed for the new conditions, the control effort required by the feedback error-learning scheme is usually high when compared to the adaptive neural controllers [25].

Most of the present works on neural network based adaptive control are on full scale models, though there have been attempts to design flight control systems for subscale unmanned air vehicles (UAV) using conventional control approaches. UAV presents an effective test bed for flight controllers due to their inherent uncertainties in terms of modeling errors and center of gravity variations [26–30]. In our recent work [30], an indirect adaptive neural flight control scheme is developed to stabilize the unstable unmanned research aircraft (RA) and also provide necessary tracking performance. In this approach, the neural identifier and controller approximating the nominal linear plant and control law are trained off-line for finite time interval. The off-line trained neural networks are adapted online to compensate for aerodynamic modeling errors and control surface failures. However, the performance of neural flight control scheme depends on the identifier model. Inaccurate identifier model can cause divergence of the neural controller network. Also the rate of adaptability of the controller and identifier networks in on-line learning affects the performance of the closed-loop system.

The main contribution of the paper is the design of direct adaptive neural control scheme that circumvents the above problems. Multilayer perceptron with linear network based adaptive controller is developed stabilize the unstable unmanned research aircraft and also track pitch rate command signal. The neural controller is adapted on-line for aerodynamic uncertainties, control surface failures and variation in the center of gravity. In order to assess the performance of the direct adaptive control scheme, the results are compared with those of indirect adaptive control scheme and also evaluated using full-scale six-degree-of-freedom model. Also, in contrast to previous works that relied on the design of conventional inner loop controller for unstable systems, the present work uses finite time training to overcome bounded signal requirement for neuron-controllers.

It is well known that small-scale aircraft are highly susceptible to wind gusts and hence difficult to control. While this aspect is often overlooked in literature, the present work provides a systematic treatment of gust disturbance specifications. The disturbance rejection capability of the neural controller is analyzed in the presence of the realistic gust and sensor noises. Hardware in loop simulation (HILS) is carried out with actuator in the loop for the nominal flight condition to test the deflection limits of actuator and to account for unmodeled nonlinear dynamics of actuator. The HILS response is compared with desktop simulation results to assess the error between the two responses. The results show the applicability of neural control scheme for practical realization.

This paper is organized as follows. Section 2 deals with the definition of the problem and describes the neural controller design procedure. Section 3 is devoted to development of research aircraft and six-degree-of-freedom model. Section 4 describes the closed-loop system specifications and Section 5 presents the numerical simulation results and hardware-in-loop simulation. Finally, Section 6 presents the conclusions.

2. Neural controller design

2.1. Problem formulation

Aircraft dynamics is represented in discrete time framework as

$$\sum : \begin{aligned} x(k+1) &= f(x(k), u(k)) \\ y(k) &= g(x(k), u(k)) \end{aligned} \tag{1}$$

where the functions $f{:}\Re^n \times \Re \to \Re^n$ and $g{:}\Re^n \times \Re \times \Re \to \Re$ are smooth and continuous, x is the vector of states, $x \in \Re^n$, u is the control input to the system, $u \in \Re$, y is the output of the system, $y \in \Re$, and k is the discrete time variable $k \in \aleph$. Without loss of generality, let us assume that the values of the functions and the inputs at equilibrium states are $f(0,0) = 0$ and $g(0,0) = 0$. The objective here is to find the control input u^* such that the aircraft response y follows the arbitrary bounded reference signal y^* belonging to the set Ω_y defined by ($y^* \in \Omega_y{:=}\{y^*{:}|y^*| \leq \Delta_2\}$, where Δ_2 is a real positive number) accurately, i.e., determine the control input $u^*(k)$, $\forall\, k > 0$ such that

$$\lim_{k \to \infty} ||y^*(k) - y(k)|| \to 0 \tag{2}$$

Let us assume that the linear system is controllable and observable at all equilibrium points along the reference signal y^* and the derivatives with respect to control input (u) is nonsingular. It follows from the implicit function theorem [31] that the control input $u^*(k)$ can be expressed in terms of past

inputs and outputs of the system.

$$u^*(k) = G(u(k-1), u(k-2), \ldots, u(k-n), y(k-1), y(k-2), \ldots, y(k-n), y^*(k+1)) \quad (3)$$

where G is a smooth and continuous function and n is the number of delays. The desired reference command signal y^* for given pilot stick deflection r is generated using the stable reference model. The reference model is selected based on the flying qualities requirements and is expressed in discrete time framework as

$$x^*(k+1) = A^* x^*(k) + B^* r(k)$$
$$y^*(k) = C^* x^*(k) \quad (4)$$

where A^*, B^*, and C^* are the system matrices.

If the reference model given in Eq. (4) is controllable and observable then the reference signal can be expressed using nonlinear autoregressive moving average model [3],

$$y^*(k+1) = H(r(k), r(k-1), \ldots, r(k-n_1), y^*(k-1), y^*(k-2), \ldots, y^*(k-n_1)) \quad (5)$$

where the function H is smooth and continuous and n_1 is the number of delays.

By substituting the Eq. (5) in Eq. (3) and assuming that the aircraft tracks the reference signal accurately, the past control inputs can be expressed in terms of pilot stick deflections and aircraft response as

$$u^*(k) = \bar{G}(r(k), r(k-1), \ldots, r(k-n_2), y(k-1), y(k-2), \ldots, y(k-n_2)) \quad (6)$$

where $\bar{G}$ is smooth continuous function and n_2 is the number of delays. The above controller is unique in the neighborhood of the equilibrium states defined earlier. Note that, the algebraic relationship given in equation (6) is valid for any bounded reference signals y^* and for any arbitrary values of inputs in the domain in which the system is controllable and observable [31].

In order to approximate the unknown function $\bar{G}$ we present a direct adaptive neural control scheme with update law based on deviation between aircraft response and desired reference command. The details of controller architecture and the update law are described below.

2.2. Direct adaptive neural controller

The block diagram of the direct adaptive neural controller is shown in the Fig. 1. $r(k)$ is the reference signal from the pilot. $e_c(k)$ is error between the pitch rate response of the aircraft ($y(k)$) and the response of the pilot filter ($y^*(k)$). The objective is to approximate the control law using neural network such that the aircraft response follows the reference command. Let us assume that the number of signals to be tracked is equal to the number of control variables. The neural network architecture shown in Fig. 2 with input $V \in \Re^{2n_2+1}$ (present stick deflection and n_2 past values of output and stick deflection) and output

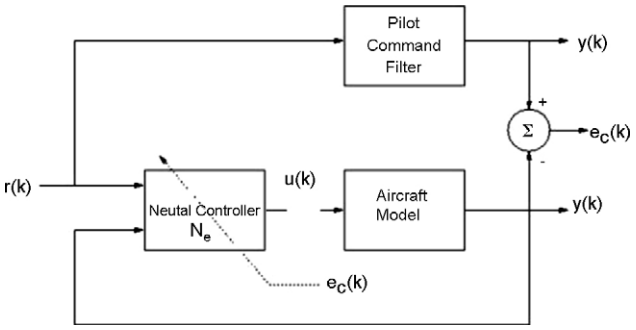

Fig. 1. Block diagram of direct adaptive neural control.

$u \in \Re$ can be represented as

$$u_{nn}(k) = w^y \sigma(w^h V) \quad (7)$$

where $w^y \in \Re^{h \times 1}$ is the weight matrix between the hidden layer and output layer with h hidden neurons, $w^h \in \Re^{2n_2+1 \times h}$ is the weight matrix between the input layer and hidden layer, and $\sigma(\cdot)$ is the activation function in the hidden layer. Among various activation functions, hyperbolic tangent function is used in this study.

The objective of the training strategy is to find the optimal weights such that the squared error between the aircraft response and the reference signal in finite horizon (finite time

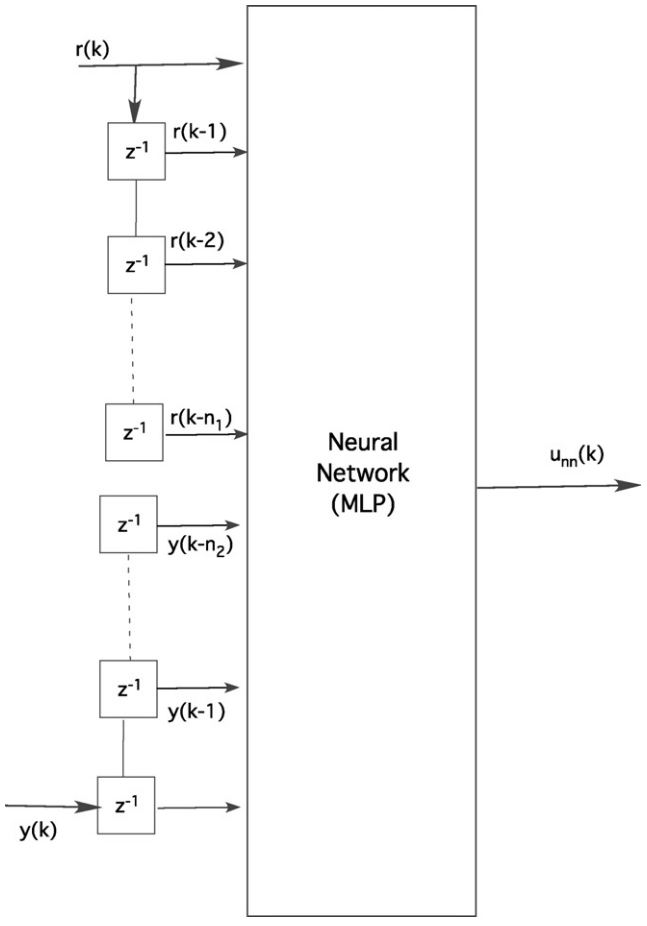

Fig. 2. Architecture of neural network.

data sequence) is minimized.

$$J = \sum_{k=1}^{N} e_c(k)^2 \tag{8}$$

where $e_c(k)$ is the difference between the actual output (target) and the network prediction at any time instant k.

$$e_c(k) = y^*(k) - y(k) \tag{9}$$

In order to adjust the weight matrices, the back propagation through time (BPTT) learning algorithm is used in this study [4].

By universal approximation property of neural networks, it is possible to approximate any function to desired accuracy if the inputs and outputs belong to compact sets. For detailed discussion on convergence of neural network parameters and robustness to initial conditions, one should refer to [32,33].

If the input to the neural network V and the output u_{nn} of the network belong to compact set, then there exist sufficient number of hidden neurons h and optimal weight matrices $\bar{w}^y$ and $\bar{w}^h$ such that the tracking error $e_c(k) < \varepsilon$, $\forall\ k > 0$. The optimal weight matrices belongs to compact set $B(w)$.

$$\bar{w}^y, \bar{w}^h := \arg \min_{w \in B(w)} \{ \sup_{V \in \Re^{2n_2+1}} ||\bar{G}[\cdot,\cdot] - u_{nn}|| \} \tag{10}$$

The control input u_{nn} is

$$u_{nn}(k) = \bar{w}^y \sigma(\bar{w}^h V) + \varepsilon(V), \varepsilon(V) \leq \varepsilon\, \forall\, V \text{ in some input space} \tag{11}$$

Since the aircraft considered in this paper is unstable, the response of the aircraft may grow unbounded for bounded elevator input, i.e., input to the neural network V does not belong to compact set. Hence, in this paper, we propose an off-line finite horizon time learning scheme. For this purpose, let us assume that for a given class of bounded input sequence and any finite initial condition x_0, the state and output does not escape to infinity in finite time horizon.

$$\sup_{k \in [1,N]} ||y(k)|| \leq \Delta \tag{12}$$

where Δ is positive real number and N is the sequence length. Using the above assumption, we define a compact set S as

$$S := \{(r, y) \in \Re^2 : ||y(k) - y_0|| \leq \varepsilon, u \in U\}\, \forall\, k \in [1, N] \tag{13}$$

where ε is a real constant and y_0 is initial output. Hence, the input V to the neural network N_c belongs to compact set inside the finite time horizon [1, N]. Based on the above statements, we develop an off-line and on-line learning strategy. The neural network N_c is first trained off-line using the reference signal generated for finite sequence [1, N]. Such off-line trained networks can approximate the control law well within the finite sequence and stabilize the system for different initial conditions. The off-line trained controller weights are adapted on-line for various aerodynamic uncertainty and control surface fault conditions.

3. Research aircraft

3.1. Aircraft configuration

The unmanned aircraft considered for this study, research aircraft (RA), is shown in Fig. 3. The model features a tailless delta wing configuration typical of a combat aircraft. The take off weight of RA is approximately 5.5 kg and is powered by a ducted fan driven by a 15-cc piston engine (OS91) with an achievable RPM of approximately 18,000. The fuel used is a mixture of methanol and castor oil with nitro-methane added to boost the power. The servos used for control surface deflection are FUTABA radio-controlled servos.

3.2. Aircraft dynamics and modeling

Based on the assumption of the flat Earth, constant mass properties, and following the symbols and definition used in [34], the generic equations of translational and rotational motion of aircraft dynamics can be expressed as

$$\dot{x} = f(x, u, t) \tag{14}$$

The above system of nonlinear equation describing the aircraft dynamic behavior is known to us reasonably and accurately as a mix of analytic expressions and tabular data [34]. It should be noted that this equation describes the fully six-degree-of-freedom nonlinear motion of an aircraft in three-dimensional space. The complexity of the equations of motion is further increased due to the nonlinearity of and coupling with the aerodynamic forces and moments. The elements of body-axes state vector (x) are U, V and W, which represent the velocity along x, y and z body axes respectively, P, Q and R, representing the angular rate along the x, y and z body axes respectively, ϕ, θ and ψ denoting roll angle, pitch angle and heading angle respectively, and p_x, p_y and p_z representing the North, East and Height coordinates

$$x = [U, V, W, P, Q, R, \phi, \theta, \psi, p_x, p_y, H]^{\mathrm{T}} \tag{15}$$

The aerodynamic force and moment components depend on the control surface deflections and these deflections form inputs

Fig. 3. Research aircraft.

to the aircraft model. The control vector comprises of throttle setting δ_t, elevator deflection δ_e, aileron deflection δ_a and rudder deflection δ_r.

$$u = [\delta_t, \delta_e, \delta_a, \delta_r]^T \tag{16}$$

These aerodynamic forces and moments are determined from extensive theoretical and experimental works and given in the format of a numerical look-up table. The complete aerodynamic data are acquired using low speed wind tunnel data [35] for static derivatives and analytical methods [36] for dynamic derivatives.

3.3. Control surface modeling

The control surface servo is modeled using first-order system. The transfer function between the command signal and actual deflection is modeled as a first order system:

$$\frac{\delta_e}{\delta_c} = \frac{K_a}{T_a s + 1} \tag{17}$$

where $K_a = 0.6713$ and the actuator time constant $T_a = 0.105$ s. The input to the actuator is in the form of pulse width modulated signal transmitted from the ground and the output is in radians. The neutral position of the elevator corresponds to a pulse width of 1.6 ms and varies in the range of 1.2–2.0 ms. Also, it is worth noting that the control signals computed from the control law are PWM signals. Though actuators driven by PWM signals are inherently slow and subjected to rate limits, such rate limits are not taken into account in the present work. However, the control surface deflections are sought to be kept within the experimentally determined limits of $\pm 15.6^\circ$.

3.4. Linearized longitudinal model

For obtaining a set of linear equations describing the longitudinal motion of the aircraft, the nonlinear equations of motion are numerically perturbed around the trim conditions. In this paper, the steady state, straight-and-level flight conditions at two extreme cruise speeds (25 m/s and 45 m/s) are chosen as a reference flight conditions. In the state-space model, the perturbed states of the system (x) are forward speed v in m/s, angle of attack α in rad, pitch rate q in rad/s and pitch angle θ in rad. The input δ_e of the system is the elevator deflection in radians. The continuous system and control matrices A and B at the cruise speeds are given in Table 1.

4. Closed loop specifications

4.1. Closed loop specifications

Though flying qualities specifications are not available for sub-scale aircraft, such specifications for piloted aircraft can act as a guideline with respect to which design can be done [39]. For full-scale aircraft, flying qualities evaluation is done through pilot-opinion rating scales such as the Cooper-Harper scale [40]. Accordingly, the U.S. military specifications [37], for level 1 flying qualities (excellent aircraft characteristics and pilot compensation not a factor for desired performance) state that the short period (ξ_{sp}) damping requirement is: $0.35 < \xi_{sp} < 1.3$ and the short period frequency (ω_{nsp}) specification is given in terms of variation of aircraft load factor with angle of attack. For RA, this translates into: $1.43 < \omega_{nsp} < 6.42$.

4.2. Reference model selection

The pilot stick deflection (reference input) to command signal transfer function is selected based on flying quality requirement (level 1 handling quality) outlined above. The neural flight controller is designed to track the pitch rate (q^*) command signal. The reference model for pilot stick deflection is given in Table 1. The frequency and damping of the reference model is 2.24 rad/s and 0.89 which satisfy the short period specification. The dc gain of the reference model is 0.611 which means that for a PWM signal of width 0.1 ms (with respect to the neutral PWM signal of 1.6 ms), the desired pitch rate is 3.5°/s. A large pitch rate is consciously avoided, since RA is controlled from the ground based on visual cues and reaction time of the pilot is high.

4.3. Gust disturbance rejection

Subscale aircraft like RA are highly susceptible to atmospheric turbulence that commonly occurs during flight. In order to determine the gust rejection specifications of the closed loop

Table 1
System and control matrices at 25 m/s and 45 m/s cruise speeds and reference model

Trim cruise speed	A	B		Eigen values
25 m/s	$\begin{bmatrix} \mathbf{-0.1688} & \mathbf{0.8500} & 0 & -9.81 \\ \mathbf{-0.03} & \mathbf{-3.2797} & \mathbf{0.9188} & 0 \\ 0 & \mathbf{2.21} & \mathbf{-2.7546} & 0 \\ 0 & 0 & 1 & 0 \end{bmatrix}$	$\begin{bmatrix} -0.4783 \\ -0.6178 \\ -3.2529 \\ 0 \end{bmatrix}$		$\begin{bmatrix} -4.4742 \\ -1.4424 \\ -0.4915 \\ 0.2050 \end{bmatrix}$
45 m/s	$\begin{bmatrix} -2026 & 1.224 & 0 & -9.81 \\ -0.03 & -3.9357 & 0.9188 & 0 \\ 0 & 3.1824 & -3.3055 & 0 \\ 0 & 0 & 1 & 0 \end{bmatrix}$	$\begin{bmatrix} -0.6888 \\ -0.7414 \\ -4.6842 \\ 0 \end{bmatrix}$		$\begin{bmatrix} -5.3649 \\ -1.7786 \\ -0.4976 \\ 0.1973 \end{bmatrix}$
Reference model	A_{ref}	B_{ref}	C_{ref}	$-1.9936 \pm 1.021i$
	$\begin{bmatrix} -3.5392 & -2.5088 \\ 2 & 0 \end{bmatrix}$	$\begin{bmatrix} 2 \\ 0 \end{bmatrix}$	$[0.8864 \quad 0.7664]$	

system, the vertical wind gust noise is taken to have a spectral density given in Dryden form as [37]:

$$\Phi_w(\omega) = \frac{2L_w\sigma^2}{\pi U}\,\frac{1+12(L_w/U)^2\omega^2}{\left(1+4(L_w/U)^2\omega^2\right)^2} \quad (18)$$

where ω is the frequency in rad/s, σ the turbulence standard deviation, L_w the turbulence scale length and U is the flight velocity. The turbulence scale length at 1200 m altitude is $L_w = 265$ m [37].

The turbulence standard deviations are defined in statistical terms and classified as light, severe and moderate, with $\sigma = 1.55$ m/s for light wind, $\sigma = 3.05$ m/s for moderate wind and $\sigma = 5.96$ m/s for severe wind conditions [37]. RA is usually flown in mild or calm wind conditions and therefore a standard deviation of 2.5 m/s is chosen. The gust spectral density at the two extreme speeds is given in Fig. 4. The frequency range of concentration of gust disturbance is found to increase with speed and for the flight condition at 45 m/s it reaches 13 rad/s. This represents the worst-case scenario when disturbances may excite the short period mode. Taking this as the benchmark, the gust rejection specification is to reject all disturbances below 13 rad/s.

4.4. Noise rejection

Though the MEMS sensor used for measuring pitch rate has an inbuilt 50 Hz low pass filter, it is found that the sensor outputs are noisy and biased with noise concentration in the region above 30 rad/s. These noises coupled with the mechanical vibrations of the airframe could lead to erroneous measurements making the control of aircraft difficult. Thus high frequency specification is to reject all noise above 30 rad/s.

4.5. Robustness specifications

The offline/online trained controller should satisfy performance requirements (Level 1 flying qualities) in the entire cruise range of 25–45 m/s. The controller should also be robust to fault conditions and variations in C.G. location.

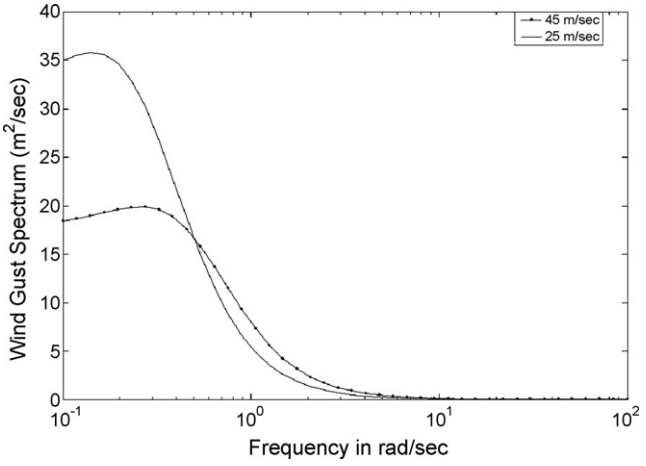

Fig. 4. Frequency response of wind spectral density for speeds of 25 and 45 m/s.

5. Simulation results

In our simulation studies, neural controller is designed to follow pitch rate command signal. The pitch stick to pitch rate command is defined based on the desired flying quality requirements. In order to train the neural controller (N_c), pseudo random pulse reference stick inputs and the desired pitch rate command signal (q^*) are generated for 10 s duration. Similarly, 20 different data sets are generated for various random reference stick signal and initial conditions. These data are used to adapt the neural controller weight matrices off-line. The input to the neural networks are present stick deflection, past two stick deflections and past four pitch rate (q) and pitch attitude (θ) responses of the aircraft. The output of the neural controller is the elevator deflection (δ_e) to the aircraft. The difference between the aircraft pitch rate response and the reference command is used to adapt the controller weight matrices. The controller network selected in our simulation study is $N_c^{11,35,1}$, i.e., 11 input neurons, 35 hidden neurons and 1 output neuron. The controller network weights are adapted until the mean square error is less than 0.002. Typical reference input to the reference command filter and response of the aircraft and actual command signal during offline training is shown in Fig. 5. From the figure, we can observe that the controller parameters adapts such that they start following reference command accurately. The results clearly indicate that the off-line trained controller parameters converge to optimal value.

5.1. Indirect adaptive control scheme

The objective of indirect adaptive control scheme is defined quantitatively as: Given an aircraft model, a reference model and a reference pilot input (r), the problem is to determine the elevator input to the aircraft (δ_e) (which will be the output of the neural network controller) so that the response of the aircraft response (q) follows the reference model (q^*). In indirect adaptive control, two neural networks namely identifier network (N_I) and controller network (N_c) are used. The identifier neural network is used to approximate the input/output relationship of the aircraft dynamics and the controller

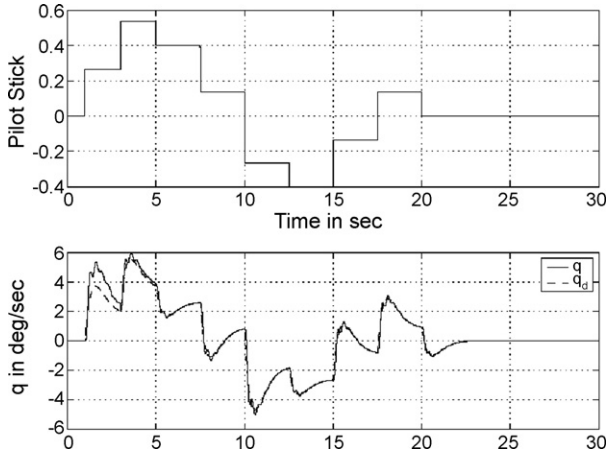

Fig. 5. Reference input to the command filter and responses during off-line training process.

network is used to approximate the unique control law that forces the aircraft output to follow the reference model output accurately. The method of indirect adaptive control relies on the ability to derive the control law given the identifier model, for a class of systems. The details on adaptive law for identifier network and controller network can be found in [3,30].

The input to the N_I are present elevator deflection, past two elevator deflections and past four pitch rate (q) and pitch attitude (θ) responses of the aircraft. The output of the identifier network is the pitch rate response (q). The difference between the aircraft pitch rate response and the identifier network is used to adapt the weight matrices of identifier network. The identifier network selected in our simulation study is $N_c^{11,45,1}$, i.e., 11 input neurons, 35 hidden neurons and 1 output neuron. The identifier network is first trained offline using finite time data set. Pseuo-random inputs to elevator and corresponding pitch rate response are used to train the identifier network. Once, the network is trained offline, the controller network is trained using offline generated reference input and command signal as explained in direct adaptive control scheme. In case of indirect adaptive control scheme, the error signal passed through identifier network to calculate the error signal to adapt the controller parameters.

5.2. Response at nominal flight conditions

The performance capability of the proposed adaptive neural flight control scheme is validated using the reference pulse stick deflection (0.1 in. stick deflection). The off-line trained neural controller is tested with the reference command signal at different trim conditions (25 m/s and 45 m/s). The response of the aircraft for the given reference command at nominal speed (45 m/s) is shown in Fig. 6(a)–(d). From the Fig. 6(c), we can clearly observe that the pitch rate response follows the pitch rate command accurately. From Fig. 6(a)–(d), we can observe that the proposed neural controller stabilizes the aircraft and also provides the necessary tracking performance. The elevator deflection required to track the pitch rate command is shown in Fig. 7 and the elevator deflection is less than the maximum limit.

The performance of the proposed neural controller is compared with the indirect adaptive control scheme. For this purpose, we measure the quantitative performance measures like maximum absolute error (MAE), root mean square error (RMSE), maximum absolute elevator deflection (MEL) and control effort and defined as

$$\mathrm{MAE} = \max|q^*(k) - q(k)| \tag{19}$$

$$\mathrm{RMSE} = \sqrt{\frac{1}{N}\sum_{k=1}^{N}(q^*(k) - q(k))^2} \tag{20}$$

$$\mathrm{MEL} = \max|\delta_e(k)| \tag{21}$$

The control effort is equal to the area under the elevator deflection curve. The performance measures are calculated for different controller schemes at different flight conditions and are given in Table 2. From table, we can observe that the proposed direct adaptive controller perform better than the other control schemes and also require lesser control effort. The same can be observed at 25 m/s flight condition.

5.3. Response under gust and sensor noise

UAVs are highly susceptible to atmospheric turbulence that commonly occurs during flight. In order to determine the gust rejection specifications of the closed loop system, the vertical wind gust noise is taken to have spectral density given in previous section. For purposes of simulating atmospheric gust, a wide band white noise is passed through the low pass filter

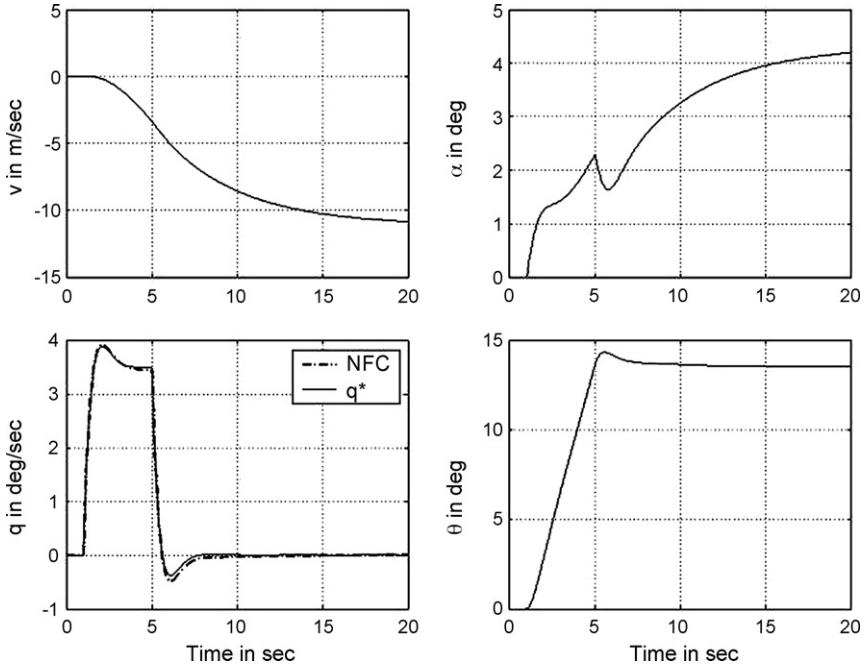

Fig. 6. Response of the aircraft at 45 m/s.

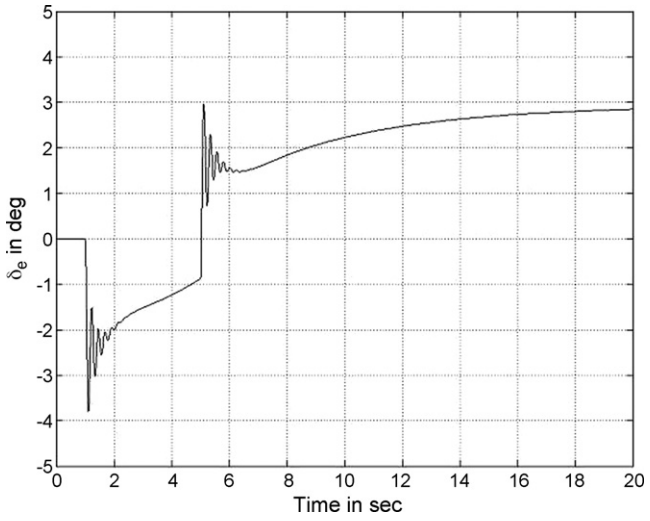

Fig. 7. Elevator deflection.

obtained from Dryden model [24].

$$H_{v_g} = \sigma_v \sqrt{\frac{2L_w}{\pi U}} \frac{(2\sqrt{3}L_w/U)s + 1}{(2L_w/Us + 1)^2} \quad (22)$$

The sensor noise is added by passing white noise through a high pass shaping filter $0.002(s + 30)/s + 100$, which corresponds to high frequency gain of 0.002. The simulation studies are carried out at 25 m/s and 45 m/s with atmospheric gust and noise in the measurement. The responses of the aircraft under gust and noise at 45 m/s (nominal flight condition) are shown in Fig. 8.

From the above figure, we can observe that the proposed neural controller reject the noise and gust very well and also the control surface deflection is within acceptable limits. The offline trained controller is also tested at 25 m/s to study the noise and gust rejection ability. The performance measures for proposed neural controller and other control schemes are calculated at these conditions and given in Table 2. From the performance measures, we can see that the proposed neural controller can accurately track the pitch rate command and also reject the gust and noise disturbances.

5.4. Response under fault conditions

In order to test the adaptive nature of the neural controller, three fault conditions are considered. The controller weights are initialized to the offline trained values and adapted online. The adaptation of controller weights starts if the performance index J (Eq. (11)) crosses a certain threshold value and the learning rate for weight update is 0.03. During this process, the reference command is generated using pseudo random inputs for a period of 100 s. After online adaptation of 100 s, the closed loop is tested using the same reference command used in offline testing.

5.4.1. C.G. variation

In the first condition, the center of gravity point of the aircraft is moved further aft of the aerodynamic center by 3%. This corresponds to an increase in M_α from 3.1824 to 4.1371. Such a variation in M_α can be caused by improper placement of hardware in the instrumentation chamber and also due to depletion in fuel during flight. It has to be noted that the class of UAVs to which RA belongs is very sensitive to such changes in center of gravity position.

The response of the closed loop system is shown in Fig. 9 for the nominal condition of 45 m/s. Sensor noise and gust disturbance are also considered in the simulation. The pitch rate response of the aircraft can be seen to track the reference pitch rate command quite well. In fact, the sensor noise and gust disturbances injected in the system are seen to be rejected completely. The small amplitude high frequency oscillations seen in the elevator response is due to the presence of sensor noise. The maximum rate of deflection of the elevator is 19°/s, which is quite low. Variation in center of gravity position for the cruise speed of 25 m/s is also carried out and it is found that the model following ability of the closed loop system is preserved. In fact, the different performance measures outlined in Table 2 give a better picture of the adaptive ability of the proposed control scheme. Under the proposed control scheme, the performance measures are better when compared to the indirect adaptive scheme. In the case of indirect adaptive control scheme, any error in the identifier model translates into degraded model matching performance [3].

Table 2
Performance measures for controller at different flight conditions

Speed, V (m/s)	Condition	Direct adaptive control					Indirect adaptive control				
		MAE (°/s)	RMSE (°/s)	MEL (°)	Control effort	Final $\lvert\delta_e\rvert$ (°)	MAE (°/s)	RMSE (°/s)	MAE (°)	Control effort	Final $\lvert\delta_e\rvert$ (°)
45	Nominal	0.4021	0.0510	3.7994	40.1221	2.7812	0.6296	0.0973	3.9189	44.2315	2.8912
	With gust and noise	0.3931	0.0515	3.7224	41.7725	2.8551	0.5153	0.1011	4.0741	45.5311	3.0121
	SMU $A = 1.5A$	0.3923	0.0696	6.5695	94.0321	6.4741	0.9145	0.1295	7.1293	103.2134	7.0145
	CSL $B = 0.5B$	0.5524	0.0880	6.8566	82.2161	5.5351	1.0524	0.1678	6.9961	91.2516	5.8311
	3% C.G. variation	0.3906	0.0587	3.7124	49.6432	3.5851	0.6123	0.0779	4.1141	53.7312	3.7866
25	Nominal	0.4763	0.0623	5.0753	55.3261	4.0123	0.6671	0.0916	5.7891	59.9864	4.4529
	With gust and noise	0.5123	0.0657	5.1012	56.2131	4.1091	0.8218	0.1071	5.8062	60.9232	4.5693
	SMU $A = 1.5A$	0.4763	0.1115	8.9602	125.281	8.8951	0.7891	0.1653	9.6312	136.542	9.9234
	CSL $B = 0.5B$	0.6536	0.1279	9.1135	107.765	7.5123	0.9012	0.1734	10.0051	119.391	8.7865
	3% C.G. variation	0.4913	0.0721	5.2152	58.3341	4.2983	0.9834	0.1108	5.9987	62.3762	4.9385

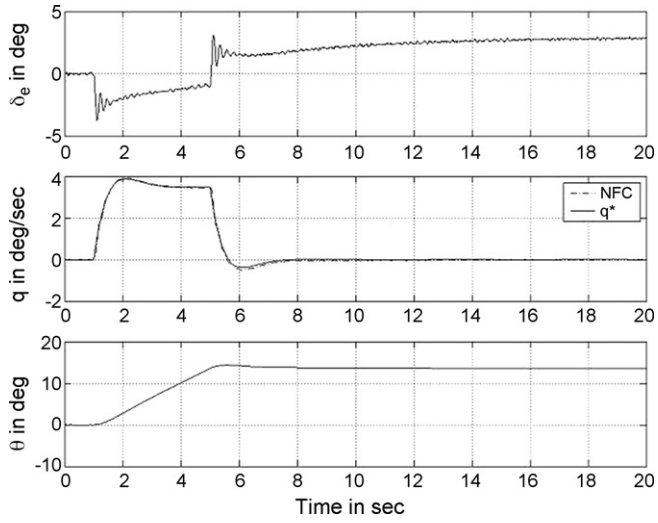

Fig. 8. Response of the aircraft under sensor noise and gust at 45 m/s.

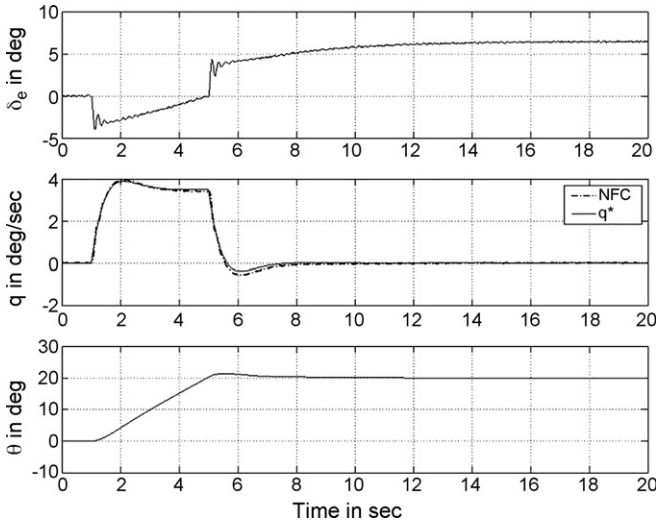

Fig. 10. Response of the aircraft under SMU fault, sensor noise and gust at 45 m/s.

5.4.2. System matrix uncertainty

In this case, the '*A*' matrix of the nominal plant is assumed to vary by 150% ($A' = 1.5A$). Since the nominal plant is unstable, an uncertainty factor of 1.5 (which is greater than 1) is chosen. This corresponds to the Eigen-values of the plant moving further into the right-half complex plane. The response of the aircraft after online adaptation is shown in Fig. 10. Again sensor noise and gust disturbance are assumed to act on the aircraft. The ability of the controller to adapt to variations in '*A*' matrix is evident from the figure, where the closed loop system closely follows the reference pitch rate command signal. Though the maximum elevator deflection is seen to be almost twice when compared to the response of the nominal closed loop system in Fig. 8, at 6.5695, the maximum elevator deflection is still less than the specified limit of 15.6°. Also, all performance measures in Table 2 show that the proposed scheme is better than the indirect adaptive control scheme.

5.4.3. Control surface loss

The third set of simulations corresponds to the case when there is sudden loss in control surface effectiveness. This is incorporated in simulations by varying the '*B*' matrix to 50% its nominal value. Fig. 11 shows the response of the closed loop system with $B' = 0.5B$ along with sensor noise and gust disturbance.

The model following properties of the closed loop system is still preserved. However, the maximum control surface deflection in this case is 6.8566, which is the maximum among all fault scenarios considered for the plant model at 45 m/s. This is quite understandable since with loss of effectiveness of the elevator, the elevator deflection required is higher to achieve better tracking. Similar studies are carried out for the extreme flight condition of 25 m/s and the performance measures are listed in Table 2.

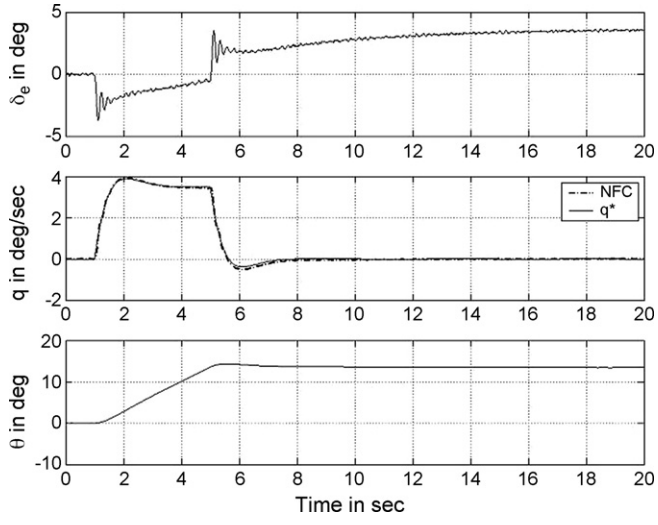

Fig. 9. Response of the aircraft under 3% C.G. variation with sensor noise and gust at 45 m/s.

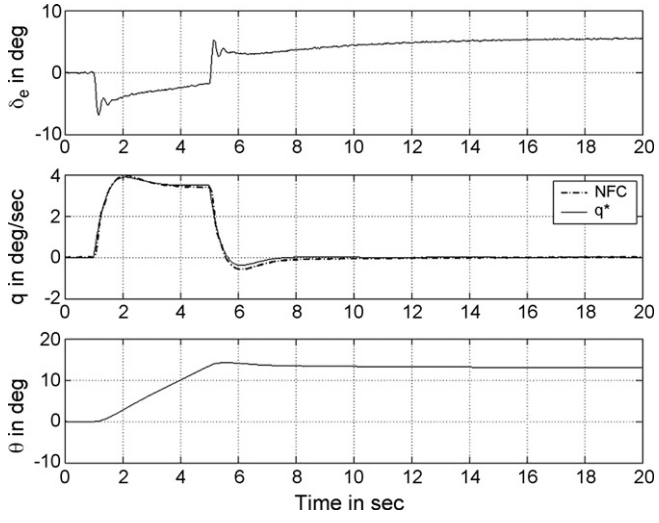

Fig. 11. Response of the aircraft under CSL fault, sensor noise and gust at 45 m/s.

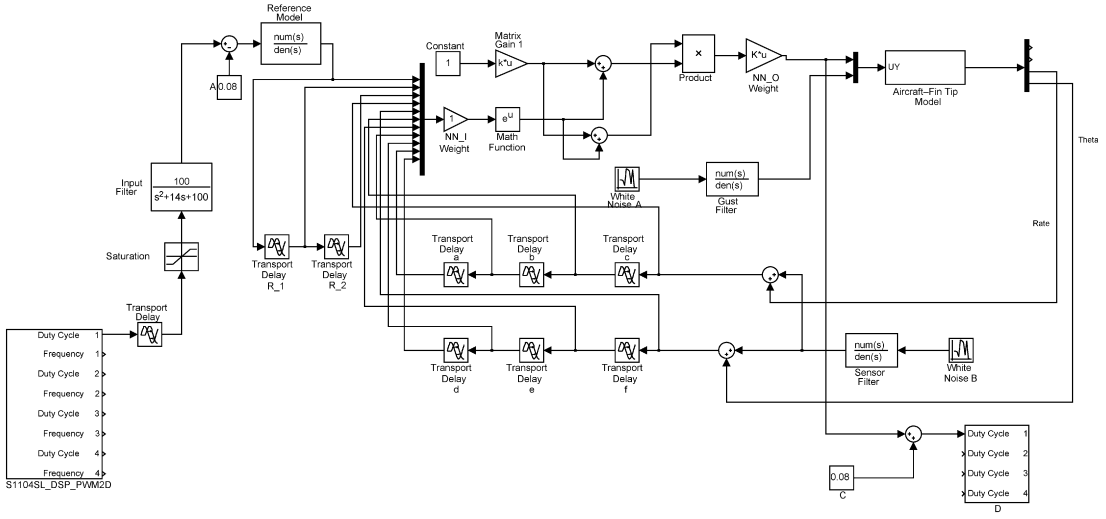

Fig. 12. HILS interconnection.

5.5. Hardware in the loop simulations

The control surface effectiveness and real time response of the aircraft to command signals from radio transmitter are tested using HILS. The requirement of testing the control surface stems from the fact that actuators are connected to the control surfaces through hard wires that can introduce nonlinearities such as backlash and dead zone. Also, there may be un-modeled friction at the control surface hinges that may affect the real time performance of the aircraft. Control surface deflection and rate limits can also be monitored in this setup.

HILS is carried out on dSPACE DS 1104 controller board with floating point processor. The controller code generated in dSPACE can easily be downloaded later for implementation on a DSP micro controller. DSPACE 1104 is interfaced to MATLAB® SIMULINK™ where the neural network controller and nominal aircraft longitudinal dynamics are modeled with a sampling time of *0.02* s. The PWM signals from transmitter (FUTABA T6XA) are captured at the capture unit of the controller board and passed through a 100 rad/s low pass filter to attenuate high frequency noise present in the input. The PWM signals entering the capture unit are of pulse width 1.2–2.0 ms with the neutral position of actuator corresponding to 1.6 ms. The neutral PWM value (trim) is deducted from the input signal to account for the fact that a linear model is being simulated. Gust and sensor noise are added at the aircraft input and sensor output to test for chattering in control surfaces and disturbance rejection capabilities of the closed loop system. The HILS interconnection is shown in Fig. 12.

The input sequence for HILS is a step command, where the pilot stick in the transmitter is moved from the initial position to one end and held for 10 s. The aircraft pitch rate response, reference command signal and elevator deflections are shown in Fig. 13 along with the command signal from the transmitter. It can be seen that the pitch rate follows that the reference output closely. Also the elevator deflection is within bounds. Gust disturbance and sensor noise are rejected completely and no chattering is observed in the elevator.

In order to test the compatibility of the results with Desktop Simulation (DKS), the same command inputs are given to the linear model. The pitch rate output of the linear model in DKS is also shown in Fig. 13. The initial variation between DKS and HILS is due to the fact that the initial command signal from the transmitter does not correspond exactly to the neutral value of the transmitter stick.

5.6. Nonlinear simulations

As a final test of the robustness of the proposed control scheme, the neural controller is used for tracking a desired pitch rate in the presence of nonlinearities. A MATLAB® based program that incorporates the nonlinear variation of force and moment coefficients is used for this purpose. The aircraft is first trimmed at 1200 m above sea level and the reference signal of 0.1 in. stick deflection is applied. Fig. 14 shows the response of the elevator deflection, reference pitch rate and actual pitch rate and pitch angle of the aircraft. As in the case of linear

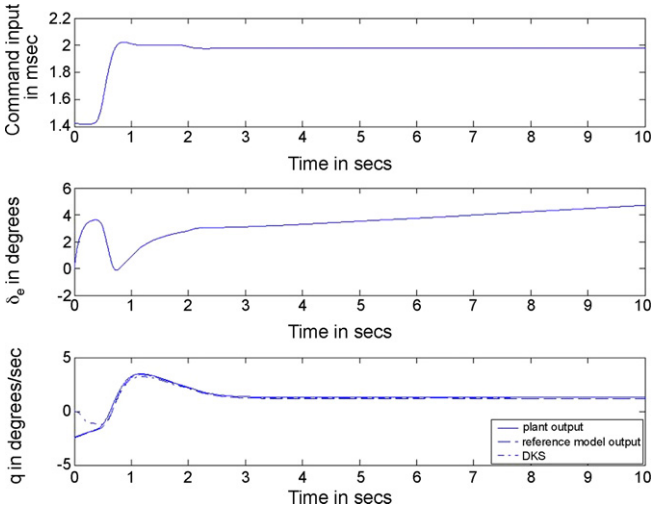

Fig. 13. HILS response.

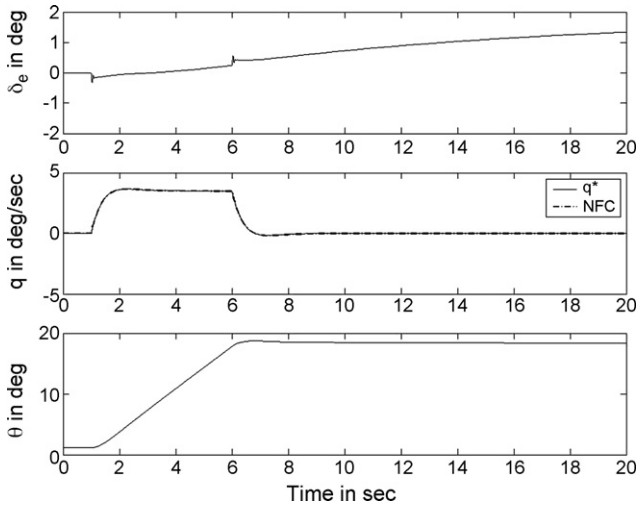

Fig. 14. Nonlinear responses.

simulations, the actual pitch rate of the aircraft follows the desired pitch rate closely. However, a notable aspect of the responses is that the elevator deflection does not reach a steady value as in the case of linear simulations due to nonlinear effects. The maximum elevator deflection is however still under acceptable limits. Thus, the proposed control scheme performs well in adapting to nonlinear effects.

6. Conclusions

A discrete time direct adaptive controller scheme is presented for an unstable unmanned aircraft. The bounded input–output requirement is overcome through the use of an offline–online training strategy. The main advantages of the proposed method can be summed up as follows:

1 The control effort required in direct adaptive scheme is lesser than that in indirect adaptive scheme.
2 Sensor noise and gust disturbance rejection properties are conserved over the entire cruise speed range with very good tracking accuracy of the reference signal, proving the robustness of the controller.
3 Control surface deflection is maintained well within saturation limits as shown in the Hardware-in-the-loop simulations.

Acknowledgement

The author would like to thank the reviewers for their valuable comments and suggestions, which has improved the quality of presentation considerably.

References

[1] Q. Zhao, J. Jiang, Reliable state feedback control system design against actuator failures, Automatica 34 (10) (1998) 1267–1272.
[2] S.A. Snell, D.F. Enns, W.L. Garrard, Nonlinear control of a super-maneuverable aircraft, in: Proceeding AIAA Guidance Navigation and Control Conference, Washington, DC, August 1989, Paper AIAA-89-3486.
[3] K.S. Narendra, K. Parthasarathy, Identification and control of dynamical systems using neural networks, IEEE Trans. Neural Netw. 1 (1) (1990) 4–27.
[4] K.S. Narendra, S. Mukhopadhyay, Adaptive control of nonlinear multivariable systems using neural networks, Neural Netw. 7 (5) (1994) 737–752.
[5] J.B.D. Cabrera, K.S. Narendra, Issues in the application of neural networks for tracking based on inverse control, IEEE Trans. Automatic Control 44 (1999) 2007–2027.
[6] G.W. Ng, Application of Neural Networks to Adaptive Control of Nonlinear Systems, Research Studies Press, Tauton, U.K., 1997, pp. 43–77.
[7] M. Marios, Polycarpou, Stable adaptive neural control scheme for nonlinear systems, IEEE Trans. Automatic Control 41 (3) (1996) 447–451.
[8] A.J. Calise, R.T. Rysdyk, Nonlinear adaptive control using neural networks, IEEE Control Syst. Mag. 18 (6) (1998) 14–25.
[9] Y. Li, N. Sundararajan, P. Sarachandran, Stable neuro-flight controller using fully tuned radial basis function neural networks, J. Guidance Control Dyn. 24 (4) (2001) 665–674.
[10] Robert M. Sanner, Jean-Jacques E. Slotine, Gaussian networks for direct adaptive control, IEEE Trans. Neural Netw. 3 (6) (1992) 837–863.
[11] A.J. Calise, M. Sharma, J.E. Corban, An adaptive autopilot design for guided munitions, in: AIAA Guidance, Navigation, and Control Conference, vol. 3, AIAA, Reston, VA, (1998), pp. 1776–1785.
[12] J. Leitner, A.J. Calise, J.V.R. Prasad, A full authority helicopter adaptive neuro-controller, in: IEEE Aerospace Conference Proceedings, vol. 2, Int. Electrical and Electronics Engineers, NY, (1998), pp. 117–126.
[13] F. Nardi, R.T. Rysdyk, A.J. Calise, Neural network based adaptive control of a thrust vectored ducted fan, in: AIAA Guidance, Navigation, and Control Conference, vol. 1, AIAA Reston, VA, (1999), pp. 374–383.
[14] M.B. McFarland, A.J. Calise, Robust adaptive control of uncertain nonlinear systems using neural network, in: Proceedings of American Control Conference, vol. 3, American Automatic Control Council, Evanston, (1997), pp. 1996–2000.
[15] B.S. Kim, A.J. Calise, Nonlinear adaptive flight control using neural networks, J. Guidance Control Dyn. 20 (1) (1997) 26–33.
[16] R.T. Rysdyk, A.J. Calise, Adaptive model inversion flight control for tilt-rotor aircraft, J. Guidance Control Dyn. 22 (3) (1999) 402–407.
[17] J. Leitner, A.J. Calise, J.V.R. Prasad, Analysis of adaptive neural networks for helicopter flight controls, J. Guidance Control Dyn. 20 (5) (1997) 972–979.
[18] Y. Li, N. Sundararajan, P. Saratchandran, Neuro-controller design for nonlinear fighter aircraft maneuver using fully tuned RBF networks, Automatica 37 (2001) 1293–1301.
[19] N. Sundararajan, P. Sarachandran, Z. Wang, Robust neuro-H-∞ controller design for aircraft auto-landing, IEEE Trans. Aerospace Electronic Syst. 40 (1) (2001) 158–168.
[20] A.J. Calise, Neural networks in nonlinear aircraft flight control, IEEE Aerospace Electronics Syst. Mag. 11 (7) (1997) 5–10.
[21] M.R. Napolitano, S. Naylor, C. Neppach, S. Pispitsos, On-line learning nonlinear neuro-controllers for restructurable control systems, J. Guidance Control Dyn. 18 (1) (1995) 170–176.
[22] A.J. Calise, S. Lee, M. Sharma, Development of a reconfigurable flight control law for tailless aircraft, J. Guidance Control Dyn. 24 (5) (2001) 675–682.
[23] T. Lee, Y. Kim, Nonlinear adaptive flight control using backstepping and neural networks controller, J. Guidance Control Dyn. 24 (4) (2001) 675–682.
[24] Dong-Ho Shin, Youdan Kim, Reconfigurable flight control system design using neural networks, IEEE Trans. Control Syst. Technol. 13 (1) (2004) 87–100.
[25] S. Suresh, S.N. Omkar, V. Mani, N. Sundararajan, Nonlinear adaptive neural controller for unstable aircraft, J. Guidance Control Dyn. 28 (6) (2005) 1103–1111.
[26] W.R. Davis, "Micro UAV," 23rd Annual AUVSI Symposium, 15–19 July 1996.
[27] R.W. Kempel, R.E. Michael, Flight control systems development and flight test experience with HiMAT research vehicles, NASA TP – 2822, June 1988.

[28] B.F. Mettler, M.B. Tischler, T. Kanade, W.C. Messner, Attitude control optimization for a small-scale unmanned helicopter, in: AIAA Guidance, Navigation, and Control Conference, 2000.
[29] J.V.R. Prasad, A.J. Calise, J. Eric Corban, Yubo Pei, Adaptive nonlinear controller synthesis and flight test evaluation on an unmanned helicopter, in: IEEE International Conference on Control Applications, 1999.
[30] S. Suresh, N. Kannan, S.N. Omkar, V. Mani, Time bounded neural network command control design for unstable aircraft, 42nd AIAA Aerospace Sciences Meeting and Exhibit, Nevada, AIAA paper no. 2004-773, 2004.
[31] Lingji Chen, K.S. Narendra, Identification and control of a nonlinear discrete-time system based on its linearization: a unified approach, IEEE Trans. Neural Netw. 15 (3) (2004) 663–673.
[32] A.R. Barron, Universal approximation bounds for superposition of a sigmoidal function, IEEE Trans. Information Theory 39 (3) (1993) 930–945.
[33] G. Cybenko, Approximation by superposition of a sigmoidal function, Math. Contr. Signal Syst. 2 (4) (1989) 303–314.
[34] B.L. Stevens, F.L. Lewis, Aircraft Control and Simulation, John Wiley and Sons, Inc, NY, 1992.
[35] S.P. Govinda Raju, K.R. Reddy, B.R. Srinivasa Rao, V. Surendranath, Experimental study of aerodynamic forces and moment characteristics in the wind tunnel on an aircraft model with thrust vector control in pitch and yaw directions, Department of Aerospace Engineering, Indian Institute of Science, Bangalore, April 2000, IWTR 278.
[36] J. Roskam, Airplane Design, Part VI: Preliminary Calculations of Aerodynamic Thrust and Power Characteristics, Roskam Aviation and Engineering Corporation, Ottawa, Kansas, 1970.
[37] Military standards for flying qualities of piloted aircraft, MIL-STD-1797A, 1990.
[39] F. Amato, U. Ciniglio, F. Corrato, R. Iervolino, μ synthesis for a small commercial aircraft: design and simulator validation, J. Guidance Control Dyn. 27 (3) (2004) 479–490.
[40] G.E. Cooper, R.P. Harper Jr., The Use of Pilot Rating in the Evaluation of Aircraft Handling Qualities, NASA TN D-5153, 1969.